Title
NEIL1 Responds and Binds to Psoralen-induced DNA Interstrand Crosslinks*

Journal
Journal of Biological Chemistry, 288(18)

ISSN
0021-9258

Authors
McNeill, Daniel R
Paramasivam, Manikandan
Baldwin, Jakita
et al.

Publication Date
2013-05-01

DOI
10.1074/jbc.m113.456087

Peer reviewed

THE JOURNAL OF BIOLOGICAL CHEMISTRY VOL. 288, NO. 18, pp. 12426–12436, May 3, 2013
Published in the U.S.A.

NEIL1 Responds and Binds to Psoralen-induced DNA Interstrand Crosslinks*[S]

Received for publication, January 23, 2013, and in revised form, February 26, 2013 Published, JBC Papers in Press, March 18, 2013, DOI 10.1074/jbc.M113.456087

Daniel R. McNeill[‡], Manikandan Paramasivam[‡], Jakita Baldwin[§], Jing Huang[‡], Vaddadi N. Vyjayanti[‡], Michael M. Seidman[‡], and David M. Wilson III[‡1]

From the [‡]Laboratory of Molecular Gerontology, Biomedical Research Center, NIA, National Institutes of Health, Baltimore, Maryland 21224 and the [§]Feinberg School of Medicine, Northwestern University, Chicago, Illinois 60611

Background: Components of base excision repair participate in the processing of psoralen-induced DNA adducts.
Results: NEIL1 glycosylase responds and binds to psoralen interstrand crosslinks, and interferes with efficient recognition and removal of these lesions.
Conclusion: NEIL1 exhibits affinity for DNA interstrand crosslinks and regulates crosslink processing.
Significance: Besides the efficiency of the canonical pathways, the abundance and composition of NEIL1 may influence responsiveness to environmental and therapeutic DNA crosslinking agents.

Recent evidence suggests a role for base excision repair (BER) proteins in the response to DNA interstrand crosslinks, which block replication and transcription, and lead to cell death and genetic instability. Employing fluorescently tagged fusion proteins and laser microirradiation coupled with confocal microscopy, we observed that the endonuclease VIII-like DNA glycosylase, NEIL1, accumulates at sites of oxidative DNA damage, as well as trioxsalen (psoralen)-induced DNA interstrand crosslinks, but not to angelicin monoadducts. While recruitment to the oxidative DNA lesions was abrogated by the anti-oxidant *N*-acetylcysteine, this treatment did not alter the accumulation of NEIL1 at sites of interstrand crosslinks, suggesting distinct recognition mechanisms. Consistent with this conclusion, recruitment of the NEIL1 population variants, G83D, C136R, and E181K, to oxidative DNA damage and psoralen-induced interstrand crosslinks was differentially affected by the mutation. NEIL1 recruitment to psoralen crosslinks was independent of the nucleotide excision repair recognition factor, XPC. Knockdown of NEIL1 in LN428 glioblastoma cells resulted in enhanced recruitment of XPC, a more rapid removal of digoxigenin-tagged psoralen adducts, and decreased cellular sensitivity to trioxsalen plus UVA, implying that NEIL1 and BER may interfere with normal cellular processing of interstrand crosslinks. While exhibiting no enzymatic activity, purified NEIL1 protein bound stably to psoralen interstrand crosslink-containing synthetic oligonucleotide substrates *in vitro*. Our results indicate that NEIL1 recognizes specifically and distinctly interstrand crosslinks in DNA, and can obstruct the efficient removal of lethal crosslink adducts.

A wide spectrum of DNA damage is generated through spontaneous decomposition, reactions with endogenously produced chemical species, and direct or indirect interactions with various exogenous agents. Some of the most common forms of DNA damage include simple base alterations, abasic sites, and single-strand breaks (1). More complex lesions, which are more typically associated with environmental or clinical DNA-damaging agents, include helix-distorting (bulky) base adducts, double-strand breaks, and intra or interstrand crosslinks (2). To prevent the genotoxic and lethal consequences of DNA damage, organisms have evolved a series of distinct, albeit interconnected, DNA repair mechanisms (3).

The base excision repair (BER)[2] pathway is the predominant system for coping with spontaneous hydrolytic, oxidative, and alkylative DNA modifications (4). Such lesions include uracil, 8-oxoguanine, 3-methyladenine, apurinic/apyrimidinic (AP) sites, and a variety of DNA single-strand break ends. Classic BER involves substrate base removal by a DNA glycosylase, incision at the resulting abasic site by an AP endonuclease, gap-filling by a DNA polymerase and sealing of the remaining nick by a DNA ligase. Although BER has traditionally been thought to recognize lesions that have little impact on overall DNA structure, recent evidence has implicated a direct involvement of BER in the processing of interstrand crosslinks (5). This damage involves the covalent linkage of the two complementary strands of DNA, thereby preventing strand separation that is required for events such as transcription and replication. Thus, interstrand crosslinks are highly toxic DNA modifications, which can promote genomic instability (6).

Some of the early data that suggested a role for BER factors in the removal of DNA lesions formed by crosslinking agents includes the mild hypersensitivities reported for homozygous 3-methyladenine DNA glycosylase (MPG)-deficient mouse cells to bis-chloroethylnitrosourea and mitomycin C (7, 8). Whether or not this increased sensitivity was the result of impaired removal of interstrand crosslinks or one of the many monoadducts formed by these compounds, however, was not determined. More recent data from the Samson laboratory

* This research was supported in whole by the Intramural Research Program at the National Institutes of Health, National Institute on Aging.
[S] This article contains supplemental Figs. S1 and S2.
[1] To whom correspondence should be addressed. Tel.: 410-558-8153; Fax: 410-558-8157; E-mail: wilsonda@mail.nih.gov.

[2] The abbreviations used are: BER, base excision repair; NAC, *N*-acetylcysteine; AP, apurinic/apyrimidinic; MPG, 3-methyladenine DNA glycosylase; UNG, uracil DNA glycosylase; DAPI, diamidino-2-phenylindole; dig-pso, digoxigenin-labeled psoralen.

indicate that MPG (also known as AAG) is important for resistance of mouse embryonic stem cells to psoralen-induced interstrand crosslinks, but not angelicin-induced monoadducts, although the exact molecular process that engages MPG has not been elucidated (9).

In a separate study, Saparbaev and co-workers found that the human DNA glycosylase, endonuclease VIII-like 1 (NEIL1), excises psoralen-induced monoadducts in duplex DNA, initiating a classic BER response involving the AP endonuclease APE1 (10). Consistently, HeLa cells depleted for NEIL1 or APE1 were shown to be hypersensitive to 8-methoxypsoralen (+UVA) exposure, a treatment scheme that creates a significant percentage of monoadduct products (10, 11). More recently, Saparbaev and co-workers found that NEIL1 can also excise an unhooked interstrand crosslink remnant within a synthetic three-stranded DNA structure, catalyzing a classic BER reaction *in vitro* (12). These data imply multiple routes of entry for NEIL1 in the psoralen crosslink response.

Unlike the above work, which suggested a role for BER components in the repair of crosslink adducts, Patrick and co-workers found that cells deficient in BER display a cisplatin-resistant phenotype, which is accompanied by enhanced excision of cisplatin-induced interstrand crosslinks (13). In particular, they demonstrated that the region around a cisplatin interstrand crosslink is susceptible to increased spontaneous decay, namely cytosine deamination, due to a local structural distortion in the duplex. This physical and chemical feature of the crosslinked DNA results in a uracil-specific BER response, which would occur near the interstrand crosslink and thus interfere with the normal repair processes *in vivo*. Consistently, the authors found that cells defective in uracil DNA glycosylase (UNG), APE1, or POLβ function, key elements of an effective BER reaction, exhibit a cisplatin-specific resistant phenotype.

Given the complex picture that is emerging regarding the role of BER in interstrand crosslink processing, we sought herein to better define the involvement of NEIL1 in the cellular response to trioxsalen (psoralen)-induced interstrand crosslinks.

EXPERIMENTAL PROCEDURES

Cells and Reagents—U2OS and HeLa cells were obtained from ATCC (Manassas, VA); mutant XPC15 and corrected XPC16 cell lines from Coriell Medical Institute (Camden, NJ); and NEIL1 knockdown and control LN428 cell lines from Trevigen (Gaithersburg, MD). Dulbecco's modified Eagle's media (DMEM) was acquired from Invitrogen Corporation (Carlsbad, CA). Vectorshield Hard Set mounting medium was obtained from Vector Laboratories (Burlingame, CA), and trioxsalen, angelicin, and *N*-acetylcysteine were from Sigma, Aldrich. The chemical design and characterization of digoxigenin-tagged trimethylpsoralen (dig-pso) has been described previously (14).

Plasmid Construction and Transfection—To generate the C-terminal fluorescently-tagged NEIL1 expression construct, the NEIL1 coding region was PCR amplified in 4% DMSO using the Hercules II Fusion Enzyme according to the manufacturer's guidelines (Stratagene, Agilent Technologies, Santa Clara, CA) with primers 5HNEIL1 (5′-CCCCAAGCTTGCCACCATGCCTGAGGGCCCCGAGCT-3′) and 3ENEIL1 (5′-CGGAATTCCAGAGGCTGAGGTCCCCTCTGGT-3′), and a cDNA template obtained from Origene (Rockville, MD; catalogue no. SC123674). The PCR product was digested accordingly and subcloned into the HindIII and EcoR1 restriction sites of either pmCherry-N1 or pAcGFP1-N1 (Clontech). Nucleotide substitutions were introduced into the WT pAcGFP-NEIL1 plasmid using the QuikChange II XL Site-directed Mutagenesis kit (Stratagene) to create the G83D, C136R, and E181K variant GFP-fusion constructs.

HeLa, U2OS, XPC15 mutant, or XPC16 complemented cells were grown in DMEM with 10% FBS, 1% penicillin/streptomycin, and 1% glutamate at 5% CO_2 and 37 °C. The designated plasmid was transfected into 200,000 cells, which had been adhered for 24 h to a 35-mm glass bottom culture dish with a 10-mm microwell (MatTek Corporation, Ashland, MA), using the Dreamfect reagent according to the manufacturer's standard protocol (OZ Biosciences, Marseille, France). In brief, 1 μg of plasmid was combined with the Dreamfect reagent and incubated at room temperature for 20 min. After this time, the mixture was added to the adhered cells for 4 h and then removed. Cells were incubated for 48 h under standard culture conditions and used to determine the intracellular localization or recruitment dynamics of the specified fluorescently tagged fusion protein. With the LN428 cell lines, an identical procedure (see above) was employed using a pEGFP-N3 vector that harbors full-length XPC (15).

Protein Intracellular Location—HeLa or U2OS cells were transfected with the indicated plasmid using the approach outlined above in slide chambers. 48 h post-transfection, the medium was removed, and cells were sealed under a glass coverslip with 50 μl of Vectorshield Hard Set mounting medium with diamidino-2-phenylindole dye (DAPI). The slides were allowed to harden overnight at 4 °C, and were viewed using a Nikon Eclipse TE2000-E microscope equipped with a CCD camera (Hamamatsu, Tokyo, Japan) and various fluorescence modules. Velocity software (Improvision, PerkinElmer, Coventry, England) was used to capture and process images. All images were acquired using identical gain, exposure, sensitivity, and contrast settings.

Protein Recruitment Dynamics—Localized microirradiation was performed using the Nikon Eclipse TE2000-E microscope set-up described above, a SRS NL100 nitrogen pumped dye laser with Micropoint ablation system (Photonics Instruments, St. Charles, IL) adjusted via passage through a dye to generate a wavelength of 365 nm, and a CSU10 spinning disk system (Yokogawa, Japan). Laser power was attenuated in terms of percent intensity using Velocity software (see above). In particular, a defined laser intensity was directed to deliver pulses to a delineated rectangular region of interest (94 $\times$ 20 pixels, 0.16 μm/pixel) using a Plan Fluor $\times$60/1.25 numerical aperture oil objective. Galvanometer-driven beam displacers oriented the laser beam, which fired randomly throughout the region until complete exposure was obtained; 300 nm was used for the diffraction limited spot size. The laser fires 3-ns pulses with a 10 Hz repetition rate with a power of 0.7 nanowatts, measured at the back aperture of the $\times$60 objective at 365 nm. A setting of 1.7% (for psoralen) and 2.2% (for angelicin) was used to create

interstrand crosslinks or monoadducts in the targeted region. A setting of 2.7% was used to create free radical induced single strand breaks (16). 30 min prior to the experiment, cells (as indicated) were treated either with 5 μM psoralen (30 min at 37 °C), 40 μM angelicin (30 min at 37 °C), or not at all. Throughout the experiment, adhered cells were maintained at 80% humidity, 5% CO_2, and 37 °C using a live cell environmental chamber or CO_2 enhancement workhead (Slonet Scientific, Segensworth, UK). Live cells were subjected to site directed laser damage at various intensities (see above). The data were analyzed using the Velocity software listed above and "region of interest fluorescent intensity" was photographically recorded as specified. All images were acquired using identical gain, exposure, sensitivity, and contrast settings.

To examine the effects of the antioxidant *N*-acetylcysteine (NAC), repair proficient HeLa cells were transfected with the pAcGFP-NEIL1 plasmid (see above) and cultured for an additional 48 h. NAC was then added to the media at a final concentration of 6 mM, and where indicated, psoralen was added 30 min prior to laser microirradiation. The cells were subsequently microirradiated at either 2.7% alone or 1.7% in the presence of psoralen. As described above, live cells were subjected to site directed laser damage and subsequent recruitment (or lack thereof) was photographically recorded. The data were analyzed, and the images were acquired as detailed above.

Western Blot Analysis—Control and NEIL1 knockdown LN428 cell lines (Trevigen) were cultured in DMEM. Once cells reached 80% confluence, they were trypsinized, washed with PBS, and harvested by centrifugation. Cell pellets were frozen at −80 °C for 1 h prior to extract preparation. Cells were re-suspended in 1 ml lysis buffer (50 mM Tris, pH 7.4, 1 mM EDTA, 1 mM DTT, 10% glycerol, 0.5 mM PMSF) and sonicated. Following centrifugation, a Bradford assay (Bio-Rad) was run to determine the protein concentration of the supernatant (whole cell extract). 30 μg of each extract was separated on a Nupage MOPS gel (Invitrogen), and the protein was transferred to a 0.2 μm PVDF membrane (Invitrogen) using standard blotting procedures. Anti-NEIL1 rabbit polyclonal antibody (Calbiochem, EMD Biosciences, San Diego, CA) was used as the primary antibody, followed by goat anti-rabbit HRP-conjugated secondary antibody (Pierce Biotechnology). Detection was carried out using a Pierce Super signal kit. β-Actin levels were determined on the same blot to ensure equal loading of whole cell extracts using a rabbit polyclonal antibody (Santa Cruz Biotechnology, Santa Cruz, CA) and the same goat anti-rabbit secondary as above. Blots were exposed to film, and all data were analyzed using ImageQuant TL software (GE Healthcare).

Colony Formation Assays—Control and NEIL1 knockdown LN428 cell lines (Trevigen) were grown to confluence, trypsinized and counted, and 100 cells were then transferred to each well of a 6-well plate. Treatments were carried out at the designated concentrations of trioxsalen (plus UVA light using a UVA Rayonet box from Southern New England Ultraviolet Company (Branford, CT)) as outlined previously (16). Cells were then gently washed twice with 1× PBS, and incubated for 10 days with fresh DMEM to allow individual colonies to form. Colonies were stained with methylene blue and counted, and the percent survival determined relative to the untreated control.

Psoralen Repair Kinetics—Control and NEIL1 knockdown cells (Trevigen) were seeded (2×10^5) in a 35-mm glass bottom culture dish for 24 h. These cells were treated with 20 μM digpso and incubated at 37 °C for 30 min prior to laser treatment at 1.7% intensity (14, 16). After the laser treatment, cells were fixed either immediately or at the indicated time point in 4% formaldehyde for 10 min at room temperature. Fixed cells were permeabilized with 0.5% Triton X-100, 1% BSA, 100 mM glycine, and 0.2 mg/ml EDTA in PBS on ice for 10 min, and subsequently digested with RNase A. Cells were blocked with 10% goat serum in PBS with 0.01% sodium azide for 1 h at 37 °C. Immunofluorescence staining using a primary digoxigenin antibody (Abcam, Cambridge, MA) and γH2AX antibody (Santa Cruz Biotechnology) was carried out. Secondary antibodies (Alexa Fluor goat anti-mouse and Alexa Fluor goat anti-rabbit (Molecular Probes)) were used for visualization. Approximately 20–25 cells were visualized for each time point. Mean Intensity of dig-pso from each cell at the damage site was measured (Velocity 6.01 version, Perkin Elmer) and corrected for background with background intensity from undamaged site of that respective cell.

Incision and Binding Assays—The oligonucleotides used to create the different DNA substrates were synthesized and gel purified by Integrated DNA Technologies, Inc. (San Jose, CA): 34–5OHC, CTGCAGCTGATGCGC[5OHC]GTACGGATCCCCGGGTAC; 34G, GTACCCGGGGATCCGTACGGCGCATCAGCTGCAG; D21, CCGCGGCGTACCGGCCGCGGC; and C21, TTGCCGCGGCCGGTACGCCGCGG. To generate the interstrand crosslink-containing duplex (D21/C21 ICL), 5 nmol of each D21 and C21 were annealed in TE buffer, and this 5 μM DNA solution was then incubated with 50 μM 4,5′,8-trimethylpsoralen for 1 h in the dark in 5 mM Tris (pH 7.6), 50 mM NaCl, and 0.2 mM EDTA. This mixture was subsequently irradiated for 20 min with UVA light (365 nm) on ice. The irradiated samples were purified over a DIONEX DNAPac ion exchange column on a Shimadzu HPLC system (LC-10ADvp) with a dual wavelength detector (SPD-10ADvp) and an auto injector (SIL-10AVvp). A solution of 25 mM NaOH (mobile phase A) and 1 M NaCl in 25 mM NaOH (mobile phase B) was used for separation of uncrosslinked and crosslinked DNA. A gradient of 2 min 10–50% B, 20 min 50–90% B, and 21 min 90–100% B was employed with a flow rate of 1.0 ml/min. The fractions were immediately neutralized after collection by the addition of Tris buffer, pH 7.4. The fractions containing the interstrand crosslinked DNA were pooled and desalted by dialysis in water in a 2,000 molecular weight cutoff cassette (Thermo Scientific, Rockford, IL) at 4 °C overnight and concentrated in a Speed-vac concentrator. The D21/C21 ICL substrate was 5′ end-labeled by T4 polynucleotide kinase (New England Biolabs, Beverly, MA) and [γ-^{32}P]ATP (3000 Ci/mmol, Perkin Elmer, Waltham, MA) using a standard protocol. For the 5-hydroxycytosine (5OHC) positive control substrate, the damage-containing strand was 5′ end-labeled prior to annealing to the cold complementary 34G strand. For the D21/C21 duplex that did not contain the site-specific interstrand crosslink, the C21

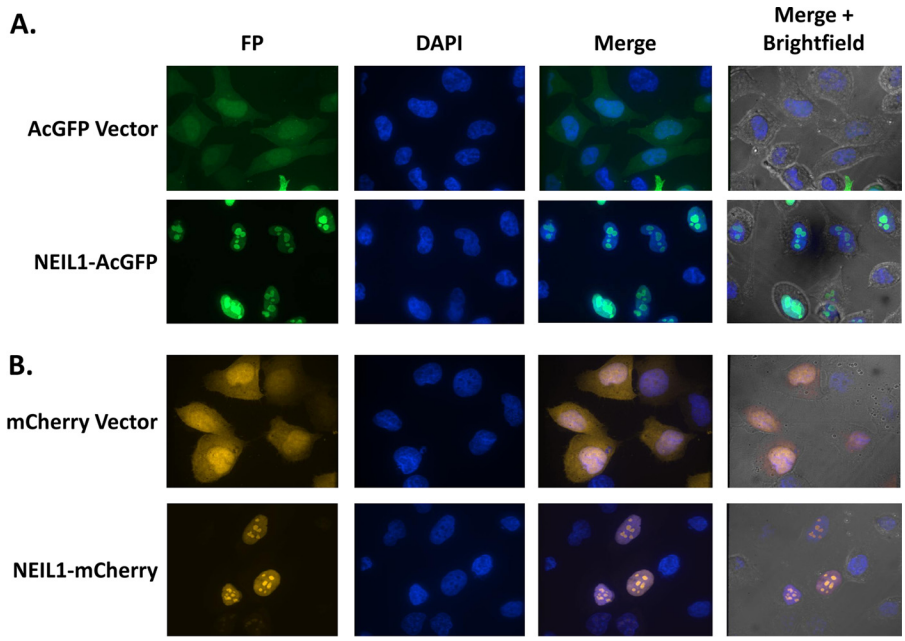

FIGURE 1. **Intracellular localization of NEIL1.** *A*, HeLa cells were transfected with either pAcGFP1-N1 or the pAcGFP-NEIL1 plasmid, fixed and stained with DAPI. Cells were then visualized and imaged for GFP or DAPI. Merge and merge plus brightfield are shown. *B*, U2OS cells were transfected with either pmCherry-N1 vector or pmCherry-NEIL1 plasmid, fixed and stained with DAPI. Cells were visualized and imaged for pmCherry, DAPI, and/or brightfield as indicated. In both *A* and *B* more than 50 cells were analyzed in this manner, and all produced similar results, with a representative field shown. *FP*, fluorescent protein.

strand was radiolabeled prior to annealing to the complementary D21 oligonucleotide.

To monitor NEIL1 glycosylase and AP lyase activities, human NEIL1 protein (New England Biolabs, Ipswich, MA) was added to a reaction mixture at the indicated amounts with 1 pmol of the appropriate oligonucleotide substrate in 10 μl of 1× endonuclease VIII buffer (New England Biolabs). After incubation at 37 °C for 10 min, the reaction was stopped by the addition of formamide loading buffer (95% formamide, 10 mM EDTA, bromphenol blue, and xylene cyanol) and heated to 90 °C for 10 min followed by incubation on ice for 3 min. The reactions were then resolved on a 20% polyacrylamide denaturing urea gel (National Diagnostics, Atlanta, GA) at 250 mV for 2.5 h. The gel was exposed to a phosphor screen (GE Healthcare, Pittsburgh, PA), which was subsequently imaged on a GE Healthcare Typhoon Trio+ Variable Mode Imager. To assess stable DNA binding, electrophoretic mobility shift assays (EMSAs) were performed by incubating NEIL1 protein (New England Biolabs) at 7.5, 22.5, or 75 ng with 100 fmol of the appropriate labeled substrate in a 10 μl volume of 70 mM MOPS, pH 7.5, 1 mM EDTA, 1 mM DTT, and 5% glycerol. Following incubation for 15 min on ice, binding reactions were resolved on an 8% polyacrylamide non-denaturing gel in TBE at 100 V for 120 min. The gel was exposed and imaged as above, and all data were analyzed using ImageQuant software (GE Healthcare).

RESULTS

Recruitment of NEIL1 to Site-specific DNA Damage—As a means of evaluating the role of DNA repair proteins in an interstrand crosslink response, we have employed a strategy whereby we transiently express fluorescent-tagged fusion proteins in human cells and monitor their recruitment dynamics to and retention time at specified sites of laser-induced DNA damage. In these experiments, photoactivated trioxsalen (psoralen) is used as the interstrand crosslinking agent, and angelicin is used as a control to generate monoadducts exclusively (Ref. 16; further details below). Our studies herein focus on the NEIL1 DNA glycosylase, since this protein has been previously shown to play multiple roles in interstrand crosslink repair (10, 12). When transiently expressed in human cervical carcinoma (HeLa) cells, NEIL1 tagged with GFP at the C terminus exhibits diffuse nuclear localization, with a significant concentration in the nucleolus (Fig. 1*A*). NEIL1 tagged with an alternative fluorescent protein (mCherry) displays a similar pattern of intracellular localization whether expressed in HeLa cells (data not shown) or human osteosarcoma U2OS cells (Fig. 1*B*).

After confirming predominantly nuclear targeting of the tagged NEIL1 protein, we determined the recruitment dynamics of GFP-NEIL1 to defined sites of DNA damage using laser microirradiation coupled with confocal microscopy. Initially, we employed a high laser dose (2.7%) known to generate DNA damage (likely oxidative lesions; see below) processed by the BER pathway to test the functionality of the GFP-NEIL1 fusion protein. As shown in Fig. 2 (*top row*), nucleoplasmic, and not apparently nucleolar, GFP-NEIL1 rapidly accumulates at the site of high dose irradiation. To determine whether NEIL1 responds to psoralen-induced adducts, pGFP-NEIL1 transfected HeLa cells were incubated with trioxsalen in culture, and then specified regions within the nucleus were targeted with laser intensities sufficient to activate the compound, but too low to produce significant oxidative lesions (1.7%). As seen in Fig. 2 (*second row*), GFP-NEIL1 was immediately recruited to sites of DNA interstrand crosslink damage (*i.e.* at the 5 s time point), dispersed completely by 8 min, and didn't re-localize to

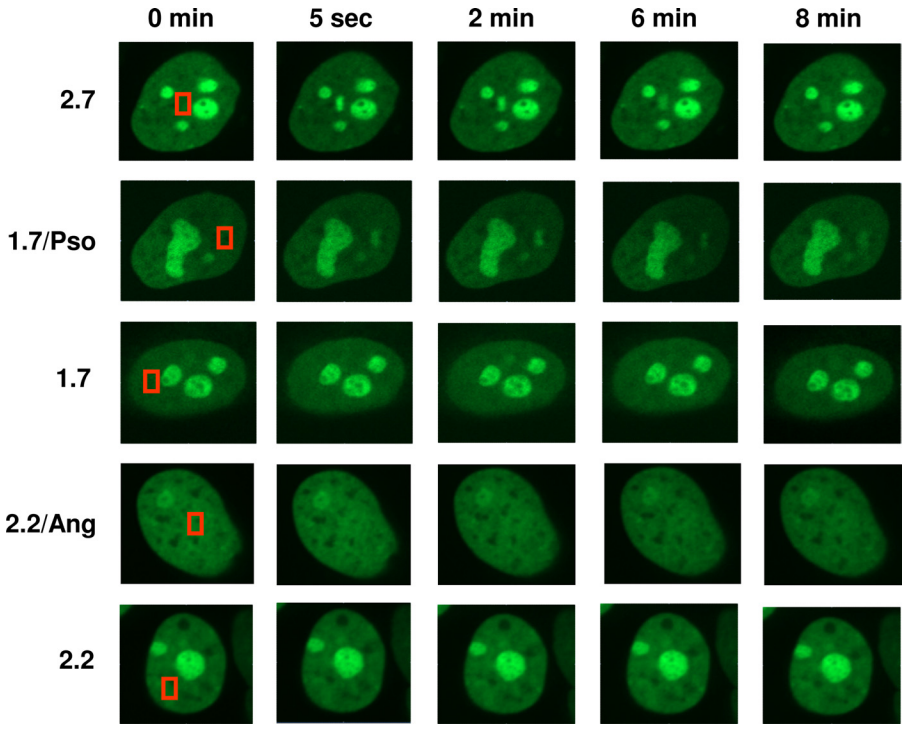

FIGURE 2. **Recruitment and retention of NEIL1 at sites of microirradiation in live cells, with or without psoralen or angelicin treatment.** HeLa cells were transfected with the pAcGFP-NEIL1 plasmid, and incubated where indicated with psoralen (*Pso*) or angelicin (*Ang*). Targeted laser treatment was then administered (area within *red box*) at the indicated intensity. Where relevant, recruitment, and dispersion kinetics of GFP-NEIL1 were recorded at the designated time points, until the GFP intensity returned to background levels. Accumulation of GFP-NEIL1 was monitored at the indicated time points in more than 50 cells under each treatment condition.

the irradiated region out to 60 min post-laser treatment (not shown). Importantly, the fusion protein did not recruit to sites treated with the low (1.7%) laser dose alone (*i.e.* no psoralen; Fig. 2, *middle row*).

To determine whether the GFP-NEIL1 response observed above is specific to psoralen-induced interstrand crosslinks and not monoadducts, we employed angelicin, a photoreactive analog of psoralen that can form only monoadducts repaired by nucleotide excision repair (NER). As depicted in Fig. 2, GFP-NEIL1 responds neither to angelicin + laser (fourth row) nor to the corresponding laser alone control (2.2%, *bottom row*), suggesting that the glycosylase is recognizing some feature specific to a trioxsalen-induced interstrand crosslink. Immunofluorescence staining with antibody against XPB confirmed that under our treatment/exposure conditions involving angelicin + laser, we were indeed generating site-specific DNA monoadducts that prompt a classic NER response (data not shown).

Role of Oxidative Damage and XPC in the NEIL1 Response—To determine the contribution of oxidative damage to the NEIL1 response reported above, we employed the anti-oxidant NAC. NAC is the *N*-acetyl derivative of the amino acid L-cysteine, and its thiol (sulfhydryl) group confers anti-oxidant effects through reduction of free radicals. We postulated that NAC treatment would abrogate any response that is reliant on the formation of oxidative DNA damage. As seen in Fig. 3*A*, NAC completely suppressed NEIL1 recruitment to sites of the high laser dose treatment (*top row*), but had no effect on the response to psoralen + low laser (*bottom row*). These results are consistent with our conclusions that the high laser dose elicits a general BER response and that the NEIL1 protein is reacting to something specific to the crosslinking agent.

Prior studies have shown that the NER damage recognition factor, XPC, which exists as part of a complex with HR23B, is an early arriver to DNA interstrand crosslink damage and directs a conventional repair response (16). To determine whether XPC facilitates the observed NEIL1 accumulation, we examined GFP-NEIL1 recruitment dynamics in cells deficient in XPC. As seen in Fig. 3*B*, GFP-NEIL1 responds similarly to psoralen + laser independent of the presence of XPC, suggesting that the glycosylase is not being recruited via the NER complex.

Silencing of NEIL1 Improves Trioxsalen Crosslink Resistance and Removal—The results of the above experiments indicate an involvement of NEIL1 in a trioxsalen-induced interstrand crosslink response. To evaluate whether NEIL1 might influence the repair of DNA interstrand crosslinks, we determined the sensitivity of control and NEIL1 shRNA lentivirus transduced LN428 glioblastoma cells to psoralen + UVA exposure. Reported quantification (Trevigen) indicates that there is an ~92% knockdown of the *NEIL1* transcript in the NEIL1 shRNA stably transduced cells as determined by RT-PCR. We performed Western blot analysis of control and NEIL1 knockdown cell extracts and found an ~72% (S.E. = 2.3%) reduction in NEIL1 protein (Fig. 4*A*). Notably, NEIL knockdown cells displayed an increased resistance to psoralen + UVA relative to the control cells as determined by colony formation assays (Fig. 4*B*), implying a negative impact of the DNA glycosylase on the resolution of cytotoxic DNA interstrand crosslink damage.

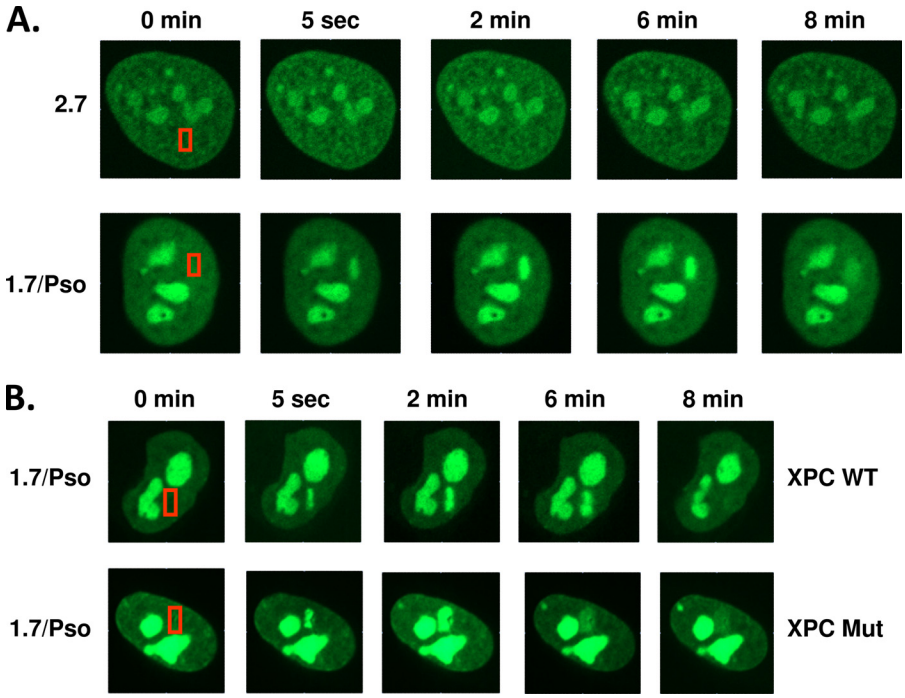

FIGURE 3. **Effect of NAC or XPC on NEIL1 recruitment.** *A*, NAC. Following transfection of HeLa cells with pAcGFP-NEIL1, cells were incubated with NAC for 30 min prior to targeted microirradiation at either 2.7% or 1.7%/Pso. Recruitment and dispersion of GFP-NEIL1 was examined at the indicated time points in more than 50 cells per treatment paradigm. *B*, XPC. XPC WT, or XPC mutant (Mut) cells were transfected with pAcGFP-NEIL1, incubated with Pso, and then microirradiated at 1.7% intensity in the presence of Pso. Accumulation of GFP-NEIL1 was monitored at the indicated time points in more than 50 cells under each treatment condition.

To examine whether NEIL1 directly affects the repair of DNA interstrand crosslinks, we monitored the removal kinetics of psoralen damage in the control and NEIL1 knockdown LN428 cell lines. In particular, the excision of psoralen adducts was followed by using a digoxigenin-labeled psoralen compound (dig-pso) as previously described (14). As shown in Fig. 4*C*, after site-specific UVA irradiation, disappearance of the labeled dig-pso compound was less efficient in the control cells in comparison with the NEIL1 knockdown cells, consistent with the idea that the glycosylase interferes with interstrand crosslink removal.

NEIL1 Binds Psoralen Interstrand Crosslink-containing DNA Substrates—Given the improved excision kinetics of psoralen-induced interstrand crosslinks and the increased psoralen + UVA resistance of NEIL1 knockdown cells, and in light of the published work by Patrick and co-workers suggesting an interfering role of BER in the cisplatin interstrand crosslink response (13), we determined whether NEIL1 displayed binding or enzymatic activity on a synthetic psoralen interstrand crosslink DNA substrate. In the initial experiments, NEIL1 was found to exhibit no noticeable glycosylase or AP lyase (strand incision) activity on psoralen interstrand crosslink-containing duplex DNA (D21/C21 ICL), while displaying significant repair activity on control 5OHC-containing double stranded substrates (supplemental Fig. S1). However, as shown in Fig. 5, we did observed stable complex formation in EMSAs of NEIL1 with the psoralen crosslinked oligonucleotide duplex, D21/C21 ICL DNA. This binding activity was not as pronounced as the positive control 5OHC substrate, but was at least 4-fold better than the non-damaged D21/C21 duplex ($p = 0.007$).

XPC Recruitment Is Enhanced in NEIL1-deficient Cells—The observation that NEIL1 binds stably to the D21/C21 ICL DNA substrate suggests a molecular mechanism for how the protein might interfere with the efficient removal of psoralen interstrand crosslinks *in vivo* (Fig. 4*C*). To explore this concept further, we determined the recruitment kinetics of a C-terminal GFP-tagged XPC to trioxsalen-induced DNA interstrand crosslinks in the control and NEIL1 knockdown LN428 cells. We reasoned that if NEIL1 binding interfered with normal damage recognition and processing, then NEIL1-deficient cells should see a more rapid accumulation of XPC at the site of the interstrand crosslink. Indeed, as seen in Fig. 6, we observed that XPC recruitment to trioxsalen crosslinks reached maximal signal intensity within the first 2 min in the NEIL1 knockdown cells, whereas maximal signal intensity was not achieved in the control cells until at least 5 min post laser irradiation. These data support the conclusion that the intracellular concentration of NEIL1 can affect substrate recognition by the XPC protein.

Response of NEIL1 Variants to Oxidative DNA Damage and Psoralen-induced Interstrand Crosslinks—NEIL1 amino acid substitution variants have been identified in the normal population and in patients with primary sclerosing cholangitis and/or cholangiocarcinoma, and some of these (*e.g.* G83D, C136R, and E181K) have been shown to exhibit impaired DNA repair activity and/or protein integrity (17, 18). In particular, the G83D variant (rs5745906; <1% frequency) was devoid of glycosylase nicking activity for most oxidative base lesions, and displayed only β-elimination AP lyase activity for pre-generated abasic sites, as opposed to the β,δ-activity seen for the

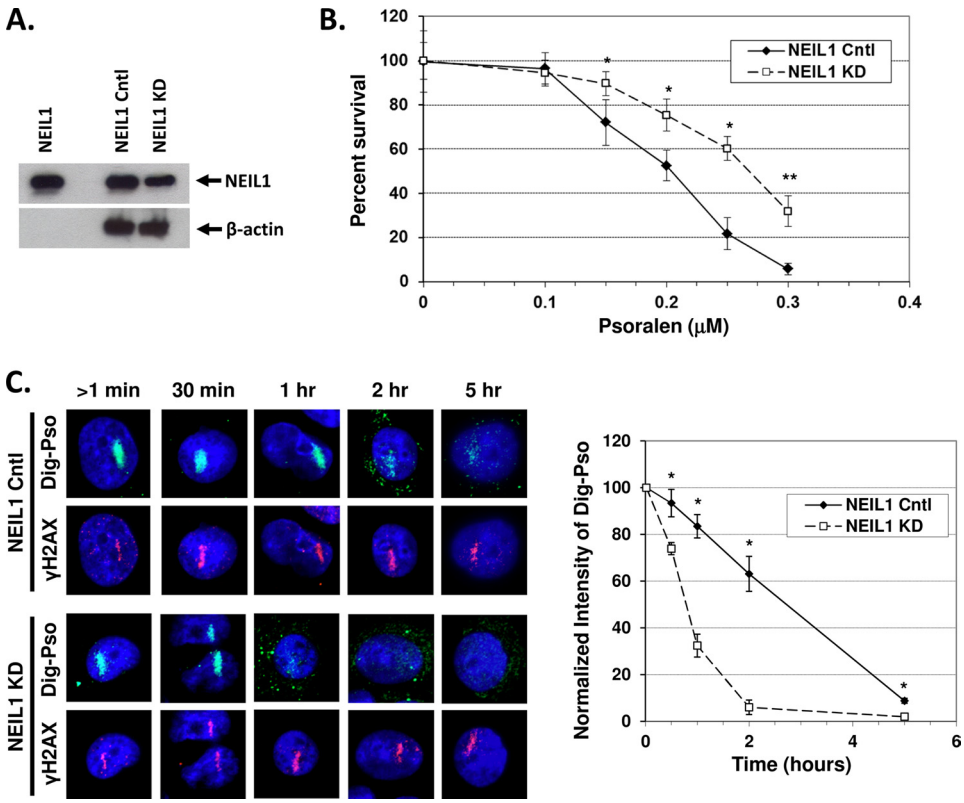

FIGURE 4. **Western blot analysis and Dig-pso repair in NEIL1 knockdown (*KD*) and control KD (*Cntl*) LN428 cells.** *A*, Western blot analysis of whole cell extracts from Cntl and KD cells, relative to purified recombinant human NEIL1 protein. Designated are the NEIL1 (*top*) and β-actin (*bottom*) signals. *B*, psoralen sensitivity. NEIL1 KD and Cntl cells were treated with the indicated doses of trioxsalen + UVA, plated, and cultured to allow for colony formation. Percent survival is plotted relative to the untreated samples, and shown is the average and standard deviation of at least 8 data points from three independent experimental runs, *, $p < 0.05$; **, $p < 0.0003$. *C*, dig-pso damage removal kinetics. LN428 KD and Cntl cells were incubated with dig-pso, and following 1.7% intensity laser treatment, the digoxigenin signal was detected and quantified at the indicated time points (*left*, images). The normalized dig-pso intensity was plotted against time, with the values shown representing the average and standard deviation of three independent experimental measurements (*right*, graph). *, $p < 0.007$. H2AX designates the region of interest to which the laser was directed. Reported *p* values were derived from ANOVA Single Factor comparative analysis of the data sets at the specified psoralen concentration or time point.

wild-type enzyme (17, 18). The C136R variant (rs5745907; <1% frequency) exhibited substantially reduced DNA glycosylase activity for oxidative base damage, and displayed inefficient and uncoupled AP lyase activity (17). The NEIL1 E181K variant (observed in 1 of 29 patients with primary sclerosing cholangitis) formed inclusion bodies when expressed in bacteria and was unable to be purified and characterized biochemically (18). We examined the intracellular distribution and recruitment dynamics to sites of high laser dose alone or to psoralen + laser of these three NEIL1 variants, as they represent possible rare altered-function susceptibility or disease-related mutants.

As shown in Fig. 7, the G83D and E181K GFP-tagged fusion proteins exhibit a similar intracellular distribution pattern as seen for WT NEIL1, *i.e.* diffuse nuclear staining with a high degree of nucleolar localization, whereas the C136R variant displays a more disperse nuclear staining pattern, and in some instances, formed noticeable spontaneous aggregates and/or had significant cytoplasmic presence (supplemental Fig. S2); a normal pattern of distribution for G83D and E181K had been reported previously (18). Recruitment studies at the high laser dose found that E181K exhibits a shorter retention time (6 min relative to 8 min for WT), that G83D displays a dramatically reduced signal intensity as well as a shorter retention time (2 min), and that C136R does not respond at all (Fig. 7, *A* and *C*). In experiments involving psoralen + laser (Fig. 7, *B* and *D*), E181K again showed a slightly shorter retention time (6 min relative to 8 min for WT), whereas G83D displayed an increased signal intensity as well as a longer retention time (12 min), and C136R exhibited a longer retention time (12 min), all relative to WT NEIL1. These data are consistent with prior studies indicating an impaired function for these variants (17, 18) and suggest that the two DNA damage responses (*i.e.* to oxidative lesions at high laser dose or interstrand crosslinks at trioxsalen + laser) involve different mechanisms of protein recruitment and retention.

DISCUSSION

In our studies here, we found NEIL1 to be a rapid responder to psoralen-induced interstrand crosslinks, belonging to a group of proteins, which have been deemed immediate early damage responders or sensors (6, 19). This seemingly instantaneous response (seen at 5 s post-irradiation for NEIL1), previously termed stage I of the repair cascade (5), likely attracts proteins that are reacting directly to a DNA modification (*e.g.* a base lesion or strand break) either independently or as part of a complex, and not to DNA processing intermediates or post-translational modifications that arise after the initial substrate recognition. XPC, a NER factor known to participate in G1 phase interstrand crosslink detection and repair, accumulates at sites of psoralen-induced DNA damage essentially

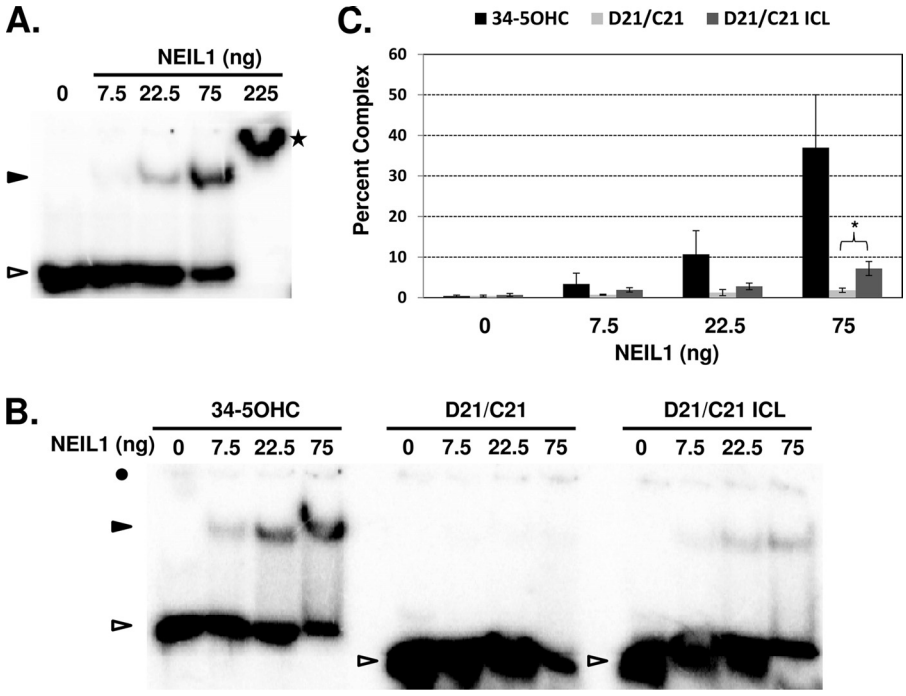

FIGURE 5. **NEIL1 binding to interstrand crosslink DNA.** *A*, NEIL1 protein titration. NEIL1 protein was incubated at increasing concentrations with the positive control 5OHC-containing duplex substrate, and the binding reactions were resolved on a native gel. *Open arrowhead*, unbound radiolabeled substrate; *closed arrowhead*, protein-DNA complex; *star*, higher molecular species, which may reflect nonspecific protein aggregation on DNA at the highest concentration. *B*, NEIL1 binding to various DNA duplexes. Binding experiments were performed as above, with the indicated DNA substrate: 34–5OHC, 5-hydroxycytosine-containing doubled stranded 34 mer; D21/C21, undamaged DNA duplex; D21/C21 ICL, psoralen interstrand crosslink-containing DNA. *Filled circle*, position of the well. *C*, quantification of the percent radiolabeled DNA bound. Data shown are the averages and standard deviations of three independent experimental measurements. *, $p = 0.007$; derived from ANOVA Single Factor comparative analysis of the specified data sets.

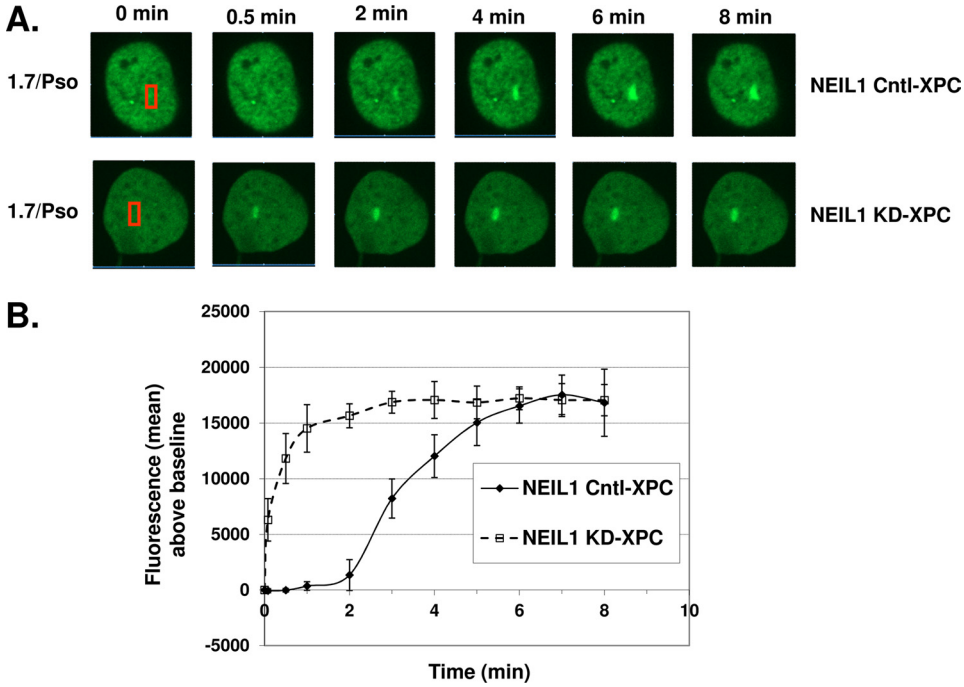

FIGURE 6. **Recruitment of XPC in NEIL1 knockdown (*KD*) and control (*Cntl*) LN428 cells.** Following transfection with p2BAC.XPChd, NEIL1 KD (labeled NEIL1 KD-XPC) and Cntl (labeled NEIL1 Cntl-XPC) cells incubated with trioxsalen were laser irradiated at 1.7% (1.7/Pso) at the indicated position. *A*, representative cell images of XPC-GFP recruitment at the indicated time points. *B*, the signal intensity at the indicated time points (average and standard deviation) is derived from 10 independent cells.

immediately (16), like NEIL1. However, XPC persists at these laser-induced interstrand crosslink foci for up to an hour, whereas NEIL1 disappears by 8 min. The difference in their persistence profiles and the fact that NEIL1 accumulates in the absence of XPC would seem to indicate that the glycosylase is not directly involved in the repair of the interstrand crosslink, but instead is attracted to a unique feature of the crosslinked DNA.

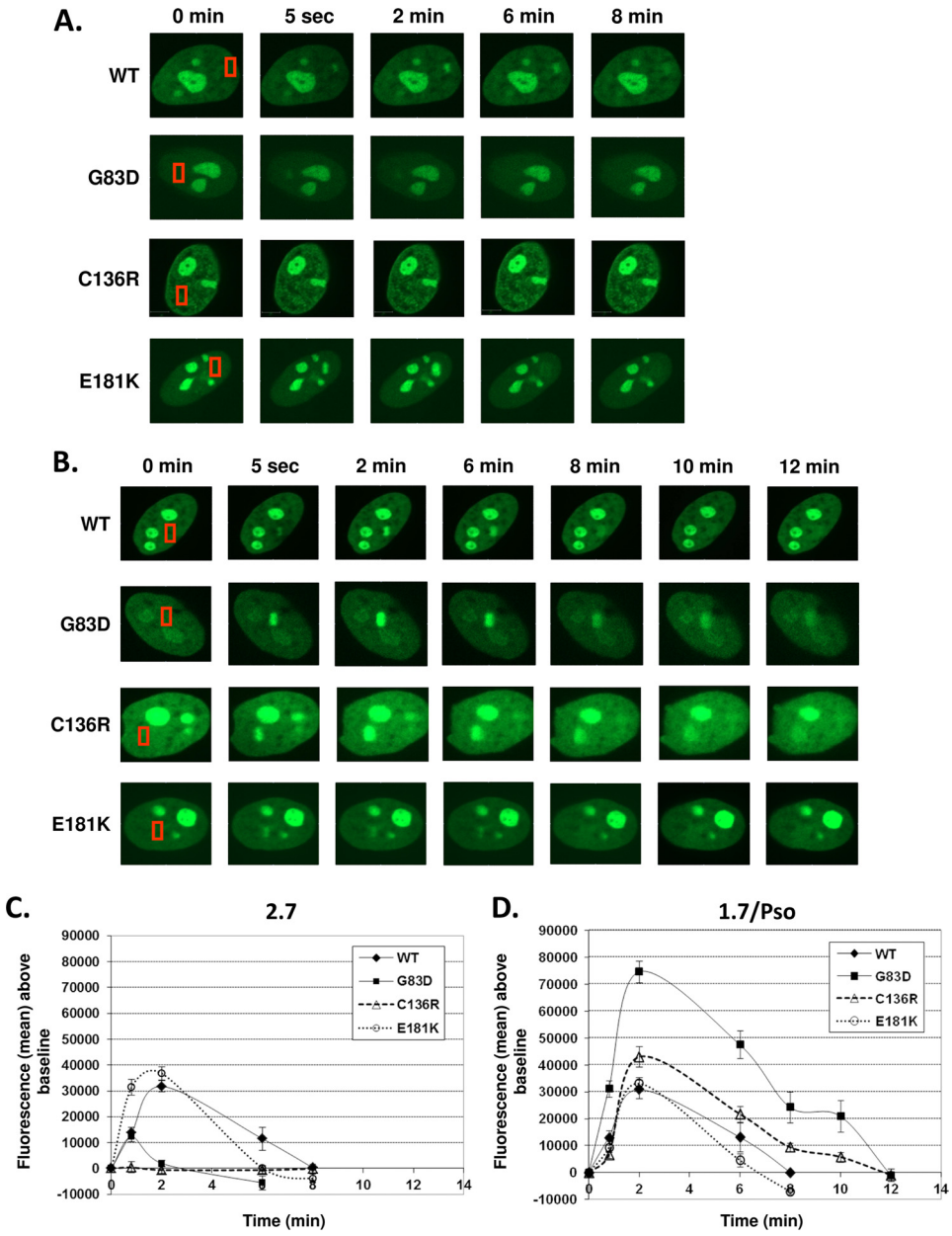

FIGURE 7. **Recruitment of NEIL1 variants to regions of targeted microirradiation.** HeLa cells were transfected with either WT NEIL1 or one of the NEIL1 variant plasmids: C136R, E181K, or G83D. Recruitment and dispersion of the different GFP-NEIL1 proteins were recorded at 2.7% (*panel A*) or 1.7%/Pso (*panel B*) at the indicated time points until intensity reached background levels. More than 50 cells per treatment were analyzed in this manner. The fluorescence above baseline was calculated for each of the above proteins at 2.7% (*panel C*) or 1.7%/Pso (*panel D*). Shown are the averages and standard deviations of results obtained from 10 independent cells.

Our observation that NEIL1 binds with higher affinity to psoralen interstrand crosslink-containing duplex DNA (D21/C21 ICL) than undamaged DNA (D21/C21) indicates some specificity of the protein for crosslink damage. While at present it is unclear what attribute of the interstrand crosslink duplex NEIL1 is recognizing, the glycosylase has been shown to exhibit increased activity on base lesions within DNA bubble structures (20). Notably, prior work has found that psoralen interstrand crosslinks can promote a local DNA structural change, with potential helix unwinding (21), possibly creating a binding site for stable NEIL1 complex formation, such as an undamaged flipped-out base. It is also feasible that such structural distortions could make the region around the interstrand crosslink prone to oxidation *in vivo*, resulting in an even more favorable substrate for NEIL1 binding. Although our biochemical assays have not revealed NEIL1 incision activity on psoralen interstrand crosslink substrates, an observation that appears consistent with prior experimental work (10), enzymatic processing by the glycosylase at or near the interstrand crosslink site *in vivo* cannot be excluded. Thus, whether the NEIL1 protein response is part of a more general BER process intracellularly is unknown.

NEIL1 exhibits a nearly identical kinetic profile in response to both oxidative DNA damage (high laser dose) and psoralen interstrand crosslinks (trioxsalen + laser). However, these responses are clearly distinct, as NEIL1 recruitment to only the

high laser dose was abrogated by treatment with the anti-oxidant NAC. This finding supports the notion that the glycosylase is recognizing something unique about the crosslinked duplex, and not simply oxidative base modifications in DNA. Moreover, it is noteworthy that the two NEIL1 protein variants known to have substantially reduced DNA glycosylase activity, G83D and C136R (17, 18), have little or no response to the high laser exposure, yet retain a near normal, even more intense response to trioxsalen + laser. This observation is consistent with (i) the high laser dose creating substrate lesions for BER enzymes (*i.e.* oxidative DNA damage) and (ii) the two responses involving a distinct NEIL1 recognition mechanism that can be uncoupled via specific mutations. Moreover, our results support the notion that these two rare reduced-function population variants, G83D and C136R, may influence disease risk, particularly for clinical conditions that involve oxidative stress and associated base lesions. The fact that we observed a near normal response for the disease-associated E181K variant may imply that this protein exhibits essentially WT repair activities, a feature that was not assessable biochemically due to the formation of inclusion bodies when expressed in bacteria (18). We note that neither the oxidative damage nor the interstrand crosslink response appears to involve DNA replication, since all cells analyzed within the unsynchronized population displayed similar NEIL1 response kinetics.

Our observations that NEIL1 deficiency leads to a more rapid excision of psoralen-induced DNA damage and increased resistance to psoralen + UVA is seemingly inconsistent with prior studies suggesting a role for NEIL1 and BER in psoralen monoadduct or crosslink remnant excision (10, 12). While the exact reason for this apparent discrepancy is unknown, it could reflect differences in the cellular background and/or the use of 8-methoxypsoralen in the earlier work, as this agent, unlike trioxsalen (which was employed herein) generates an obligate 20% monoadducts; trioxsalen, conversely, produces crosslinks at a 56:1 ratio in comparison to monoadducts (<2%) (11).[3] Although we did not observe recruitment to angelicin, our studies cannot completely exclude the possibility that NEIL1 has a role in psoralen monoadduct repair, as this was not explicitly addressed. However, since we did not see a stage II response for NEIL1 to psoralen-induced DNA damage, which should occur around 10 min post-irradiation as defined by recruitment of XPE to sites of psoralen interstrand crosslinks (16), our studies do not support a role for the glycosylase in remnant processing *in vivo*. It seems likely that proteins such as the damage-specific DNA binding factor, DDB1, a key marker for the second stage of the repair process (16), would outcompete NEIL1 in cells. We emphasize that none of our experiments rule out the possibility that NEIL1 excises psoralen monoadducts or interstrand crosslink remnants from three-stranded DNA structures *in vitro*.

In total, our results suggest a model whereby NEIL1 arrives early at the site of the psoralen interstrand crosslink, forms a stable complex at this location, and interferes with the main processes of crosslink resolution (*i.e.* NER and recombinational repair, including XPC recruitment), leading to slower crosslink removal and increased sensitivity to trioxsalen + UVA. This model is broadly consistent with the model of Patrick and colleagues, who based on a series of biochemical and cell biology experiments proposed that, upon cytosine deamination near a cisplatin interstrand crosslink, a uracil-directed BER response will hamper the normal cellular repair processes for the crosslink damage (13). Our studies indicate an interfering role for the NEIL1 glycosylase in the repair of psoralen-induced DNA interstrand crosslinks that involves binding at the crosslink site, seemingly without the formation of a cognate substrate. Future work will need to determine whether the NEIL1 response described herein is unique to psoralen crosslinks or whether other crosslinking agents can generate comparable binding sites for stable NEIL1 complex formation.

It is interesting to note that historically most studies aimed at identifying pathways involved in crosslinking agent resistance have selected for clones that are resistant to the damaging compound and then searched for up-regulated genes. As such, genes that when down-regulated play an important role in resistance would have been missed. In light of the results herein and of Patrick and co-workers (13), it seems reasonable to predict that down-regulation of specific DNA glycosylases will give rise to crosslinking agent resistance. Thus, it would seem to be worthwhile to return to earlier experiments and ask whether any of the resistant clones show significant reductions in DNA glycosylase gene expression. Moreover, in addition to providing a potential means of resistance to crosslinking agents, decreased expression of a repair glycosylase could provide a selective advantage for cell survival in the form of a mutator phenotype. Specifically, reduced DNA glycosylase activity would result in base damage accumulation and the potential for mutagenic replicative events, some of which could aid in rapid adaptation and the development of therapeutic agent resistance. Going forward, it seems reasonable that besides defining the repair capacity of the canonical interstrand crosslink responses, namely the NER factors XPF/ERCC1 and homologous recombination (22), the levels of DNA glycosylases should be considered when predicting patient responsiveness to crosslinking drugs used in the clinic. Significantly, NEIL1 protein levels and activity have been shown to be altered (primarily decreased) in cancer cells, due to both genetic and epigenetic factors (23, 24).

Acknowledgments—We thank Drs. Marina Bellani and Peter Sykora for critical reading of and helpful comments on the manuscript.

[3] D. M. Wilson, unpublished observations.

REFERENCES

1. Lindahl, T. (1993) Instability and decay of the primary structure of DNA. *Nature* **362,** 709–715
2. Stone, M. P., Huang, H., Brown, K. L., and Shanmugam, G. (2011) Chemistry and structural biology of DNA damage and biological consequences. *Chem. Biodivers.* **8,** 1571–1615
3. Jackson, S. P., and Bartek, J. (2009) The DNA-damage response in human biology and disease. *Nature* **461,** 1071–1078
4. Wilson, D. M., 3rd, and Bohr, V. A. (2007) The mechanics of base excision repair, and its relationship to aging and disease. *DNA Repair* **6,** 544–559
5. Wilson, D. M., 3rd, and Seidman, M. M. (2010) A novel link to base excision repair? *Trends Biochem. Sci.* **35,** 247–252

6. Muniandy, P. A., Liu, J., Majumdar, A., Liu, S. T., and Seidman, M. M. (2010) DNA interstrand crosslink repair in mammalian cells: step by step. *Crit. Rev. Biochem. Mol. Biol.* **45,** 23–49
7. Engelward, B. P., Dreslin, A., Christensen, J., Huszar, D., Kurahara, C., and Samson, L. (1996) Repair-deficient 3-methyladenine DNA glycosylase homozygous mutant mouse cells have increased sensitivity to alkylation-induced chromosome damage and cell killing. *EMBO J.* **15,** 945–952
8. Allan, J. M., Engelward, B. P., Dreslin, A. J., Wyatt, M. D., Tomasz, M., and Samson, L. D. (1998) Mammalian 3-methyladenine DNA glycosylase protects against the toxicity and clastogenicity of certain chemotherapeutic DNA cross-linking agents. *Cancer Res.* **58,** 3965–3973
9. Maor-Shoshani, A., Meira, L. B., Yang, X., and Samson, L. D. (2008) 3-Methyladenine DNA glycosylase is important for cellular resistance to psoralen interstrand cross-links. *DNA Repair* **7,** 1399–1406
10. Couvé-Privat, S., Macé, G., Rosselli, F., and Saparbaev, M. K. (2007) Psoralen-induced DNA adducts are substrates for the base excision repair pathway in human cells. *Nucleic Acids Res.* **35,** 5672–5682
11. Lai, C., Cao, H., Hearst, J. E., Corash, L., Luo, H., and Wang, Y. (2008) Quantitative analysis of DNA interstrand cross-links and monoadducts formed in human cells induced by psoralens and UVA irradiation. *Anal. Chem.* **80,** 8790–8798
12. Couvé, S., Macé-Aimé, G., Rosselli, F., and Saparbaev, M. K. (2009) The human oxidative DNA glycosylase NEIL1 excises psoralen-induced interstrand DNA cross-links in a three-stranded DNA structure. *J. Biol. Chem.* **284,** 11963–11970
13. Kothandapani, A., Dangeti, V. S., Brown, A. R., Banze, L. A., Wang, X. H., Sobol, R. W., and Patrick, S. M. (2011) Novel role of base excision repair in mediating cisplatin cytotoxicity. *J. Biol. Chem.* **286,** 14564–14574
14. Thazhathveetil, A. K., Liu, S. T., Indig, F. E., and Seidman, M. M. (2007) Psoralen conjugates for visualization of genomic interstrand cross-links localized by laser photoactivation. *Bioconjug. Chem.* **18,** 431–437
15. Hoogstraten, D., Bergink, S., Ng, J. M., Verbiest, V. H., Luijsterburg, M. S., Geverts, B., Raams, A., Dinant, C., Hoeijmakers, J. H., Vermeulen, W., and Houtsmuller, A. B. (2008) Versatile DNA damage detection by the global genome nucleotide excision repair protein XPC. *J. Cell Sci.* **121,** 2850–2859
16. Muniandy, P. A., Thapa, D., Thazhathveetil, A. K., Liu, S. T., and Seidman, M. M. (2009) Repair of laser-localized DNA interstrand cross-links in G1 phase mammalian cells. *J. Biol. Chem.* **284,** 27908–27917
17. Roy, L. M., Jaruga, P., Wood, T. G., McCullough, A. K., Dizdaroglu, M., and Lloyd, R. S. (2007) Human polymorphic variants of the NEIL1 DNA glycosylase. *J. Biol. Chem.* **282,** 15790–15798
18. Forsbring, M., Vik, E. S., Dalhus, B., Karlsen, T. H., Bergquist, A., Schrumpf, E., Bjørås, M., Boberg, K. M., and Alseth, I. (2009) Catalytically impaired hMYH and NEIL1 mutant proteins identified in patients with primary sclerosing cholangitis and cholangiocarcinoma. *Carcinogenesis* **30,** 1147–1154
19. Ciccia, A., and Elledge, S. J. (2010) The DNA damage response: making it safe to play with knives. *Mol. Cell* **40,** 179–204
20. Dou, H., Mitra, S., and Hazra, T. K. (2003) Repair of oxidized bases in DNA bubble structures by human DNA glycosylases NEIL1 and NEIL2. *J. Biol. Chem.* **278,** 49679–49684
21. Spielmann, H. P., Dwyer, T. J., Hearst, J. E., and Wemmer, D. E. (1995) Solution structures of psoralen monoadducted and cross-linked DNA oligomers by NMR spectroscopy and restrained molecular dynamics. *Biochemistry* **34,** 12937–12953
22. Deans, A. J., and West, S. C. (2011) DNA interstrand crosslink repair and cancer. *Nat. Rev. Cancer* **11,** 467–480
23. Shinmura, K., Tao, H., Goto, M., Igarashi, H., Taniguchi, T., Maekawa, M., Takezaki, T., and Sugimura, H. (2004) Inactivating mutations of the human base excision repair gene NEIL1 in gastric cancer. *Carcinogenesis* **25,** 2311–2317
24. Chaisaingmongkol, J., Popanda, O., Warta, R., Dyckhoff, G., Herpel, E., Geiselhart, L., Claus, R., Lasitschka, F., Campos, B., Oakes, C. C., Bermejo, J. L., Herold-Mende, C., Plass, C., and Schmezer, P. (2012) Epigenetic screen of human DNA repair genes identifies aberrant promoter methylation of NEIL1 in head and neck squamous cell carcinoma. *Oncogene* **31,** 5108–5116